Available online at www.sciencedirect.com
SCIENCE DIRECT
Agricultural and Forest Meteorology 135 (2005) 124–134
AGRICULTURAL AND FOREST METEOROLOGY
www.elsevier.com/locate/agrformet

Assessment of the broadleaf crops leaf area index product from the Terra MODIS instrument

Bin Tan [a,*], Jiannan Hu [a], Dong Huang [a], Wenze Yang [a], Ping Zhang [a], Nikolay V. Shabanov [a], Yuri Knyazikhin [a], Ramakrishna R. Nemani [b], Ranga B. Myneni [a]

[a] *Department of Geography, Boston University, Boston, MA, USA*
[b] *Ecosystem Science and Technology Branch, NASA Ames Research Center, CA, USA*

Received 6 June 2005; accepted 18 October 2005

Abstract

The first significant processing of Terra MODIS data, called Collection 3, covered the period from November 2000 to December 2002. The Collection 3 leaf area index (LAI) and fraction vegetation absorbed photosynthetically active radiation (FPAR) products for broadleaf crops exhibited three anomalies (a) high LAI values during the peak growing season, (b) differences in LAI seasonality between the radiative transfer-based main algorithm and the vegetation index based back-up algorithm, and (c) too few retrievals from the main algorithm during the summer period when the crops are at full flush. The cause of these anomalies is a mismatch between reflectances modeled by the algorithm and MODIS measurements. Therefore, the Look-Up-Tables accompanying the algorithm were revised and implemented in Collection 4 processing. The main algorithm with the revised Look-Up-Tables generated retrievals for over 80% of the pixels with valid data. Retrievals from the back-up algorithm, although few, should be used with caution as they are generated from surface reflectances with high uncertainties.
© 2005 Elsevier B.V. All rights reserved.

Keywords: Broadleaf crops; Leaf area index; Terra MODIS instrument

1. Introduction

Leaf area index (LAI) and fraction of photosynthetically active radiation (0.4–0.7 μm) absorbed by vegetation (FPAR) are two of several geophysical products that are operationally produced from the MODerate resolution Imaging Spectroradiometer (MODIS), an instrument onboard the National Aeronautics and Space Administration's Terra and Aqua platforms (Justice et al., 2002). LAI and FPAR products are required to describe the exchange of fluxes of energy, mass (e.g., water and CO_2) and momentum between the surface and atmosphere (Sellers et al., 1997).

The latest version of the Terra MODIS LAI and FPAR time series is nearly 5 years long and is a compilation of the entire data series starting from February 2000 to the present. The products are generated from surface reflectance data by a radiative transfer-based algorithm that utilizes biome-specific Look-Up-Tables (Knyazikhin et al., 1998). The products must therefore be evaluated and validated for each of the biomes in order to diagnose product anomalies and devise algorithm refinements (Morisette et al., 2002; Privette et al., 2002; Cohen et al., 2003; Fensholt et al., 2004; Huemmrich et al., 2005; Tan et al.,

* Corresponding author. Tel.: +1 617 353 8845; fax: +1 617 353 8399.
E-mail address: tanbin@crsa.bu.edu (B. Tan).

0168-1923/$ – see front matter © 2005 Elsevier B.V. All rights reserved.
doi:10.1016/j.agrformet.2005.10.008

2005; Wang et al., 2004). This paper is focused on product evaluation and algorithm refinements for broadleaf crops, which is one of the six-biome classes implemented in the MODIS LAI/FPAR algorithm. Agriculture represents 13.5% of the total vegetated area (Friedl et al., 2002) and broadleaf crops comprise a little over half the cultivated area (52%). The major concentrations of this biome class are in Asia (39%), North America (22%), Europe (17%), and South America (15%).

MODIS product versions are called Collections suggesting the linkages between various products of the same generation. For instance, the LAI/FPAR algorithm uses MODIS land cover and surface reflectance products to derive LAI and FPAR products. The surface reflectance algorithm in turn uses the aerosol optical depth product to derive atmosphere-corrected surface reflectances from calibrated, geo-projected and cloud-screened MODIS radiance measurements. Collection 3 represents the first significant processing of MODIS data into products after various initial problems with instrument calibration and electronics have been resolved, and covers the 26-month period from November 2000 to December 2002 with a gap between days 161 and 184 in year 2001 due to a failure on the Terra platform. This Collection thus provided an opportunity for evaluating the initial batch of products from Terra MODIS. These efforts lead to algorithm refinements which were implemented in Collection 4 processing that started in January 2003. This paper describes this process, but with focus on broadleaf crops.

The goal of this paper is three-fold: (a) evaluate Collection 3 LAI products to diagnose product anomalies, (b) devise refinements to the algorithm for generating the next generation products, and (c) analyze Collection 4 products and test whether the Collection 3 anomalies have been satisfactorily resolved.

The paper is organized as follows. Section 2 presents a brief background on the LAI/FPAR algorithm and products. The Collection 3 LAI product from broadleaf crop pixels globally is evaluated in Section 3. A smaller region (1200 km × 1200 km) in the upper mid-west of the USA is selected for further analysis. LAI retrievals depend critically on the quality of surface reflectance data input to the algorithm—therefore, uncertainties in surface reflectance product are quantified in Section 4.1. The performance of the algorithm is then examined as a function of surface reflectance uncertainties (Sections 4.2 and 4.3). This analysis pointed to a mismatch between modeled and measured reflectances as the cause of poor algorithm performance (Section 4.4). Algorithm refinements and Collection 4 LAI product evaluation are described in Section 5. Finally, the conclusions are highlighted in Section 6.

2. MODIS LAI/FPAR algorithm and products

2.1. Algorithm inputs

The algorithm performs retrievals of LAI and FPAR from daily surface reflectance data at 1 km resolution. Currently, red (648 nm) and near-infrared (858 nm) bands are utilized because of unknown or high uncertainties in the other land bands (Wang et al., 2001). Another important input to the algorithm is the biome classification map, in which the global vegetation is stratified into six canopy architectural types, or biomes (Friedl et al., 2002). The six biomes are: (1) grasses and cereal crops, (2) shrubs, (3) broadleaf crops, (4) savannas, (5) broadleaf forests, and (6) needle leaf forests.

2.2. Algorithm

The retrievals are performed with an algorithm based on principles of radiative transfer in vegetation canopies, hereafter called the main algorithm (Knyazikhin et al., 1998). The algorithm is designed to output LAI and FPAR given sun and view directions, bidirectional reflectance factor (BRF) and their uncertainties at different spectral bands and the six-biome land cover type. The algorithm compares observed and modeled BRFs for a suite of canopy structures and soil patterns that represent an expected range of typical conditions for a given biome type. All canopy/soil patterns for which modeled and observed BRFs differ by within a specified level band-dependent uncertainty are considered as acceptable solutions. The mean values of LAI and FPAR averaged over all acceptable solutions are reported as the output of the algorithm. This algorithm may fail if input data uncertainties are high or due to deficiencies in model formulation, in which case the retrievals are generated by a back-up algorithm based on biome-specific empirical relationships between the normalized difference vegetation index (NDVI) and LAI/FPAR (Myneni et al., 1997).

2.3. LAI and FPAR products

The products are produced at 1 km spatial resolution daily and composited over an 8-day period based on the maximum FPAR value. The 8-day product is distributed to the public from the EROS Data Center Distributed Active Archive Center. The products are projected on the Integerized Sinusoidal (Collection 3) and the

Sinusoidal (Collection 4) 10° grids, where the globe is tiled into 36 tiles along the east–west axis, and 18 tiles along the north–south axis. Further details can be found in (Myneni et al., 2002).

3. Collection 3 LAI product anomalies

As mentioned previously, Collection 3 represented the first significant processing of MODIS data into various geophysical products. It covered the 26-month period from November 2000 to December 2002 and was used to evaluate the initial batch of products. Broadleaf crops constitute about 52% of the global cultivated area with major concentrations in Asia, North America, and Europe. The annual course of broadleaf crop LAI during 2001 from these regions is shown in Fig. 1. Three anomalies are apparent: (a) unrealistically high LAI values during the peak growing season from both the main and back-up algorithms, especially in North America, (b) differences in LAI seasonality between the main and back-up algorithms everywhere, and (c) the main algorithm tends to fail more often in the summer period when the crops are at full flush.

An investigation of these anomalies requires a comprehensive analysis of the inputs and Look-Up-Table entries of the algorithm. This is not feasible at the global or hemispheric scale in view of the massive amounts of data involved—the area extent of broadleaf crops is about 8.8×10^6 km^2. Therefore, the analysis is focused on one MODIS tile (h11v04) from North America, which is a 1200 km × 1200 km region in the upper mid-west, about 40% of which is broadleaf crops (Friedl et al., 2002). The first task is to ascertain that the anomalies observed at the continental scale are also seen in this tile. To that end, the annual course of Collection 3 LAI for broadleaf crops in tile h11v04 during year 2001 is shown in Fig. 2.

Peak LAI values of about 6 during the summer time are seen in the Collection 3 product. The seasonal maximum LAI near the Bondville flux tower site for year 2001 was about 4 according to FLUXNET ground measurements (WWW1). LAI values of 2.5 (July 2000) and 3.6 (August 2000) were reported by (Cohen et al., 2003) at the same site. While these values, typically measured in a small area near the flux tower, are perhaps not representative of the tile average values for this

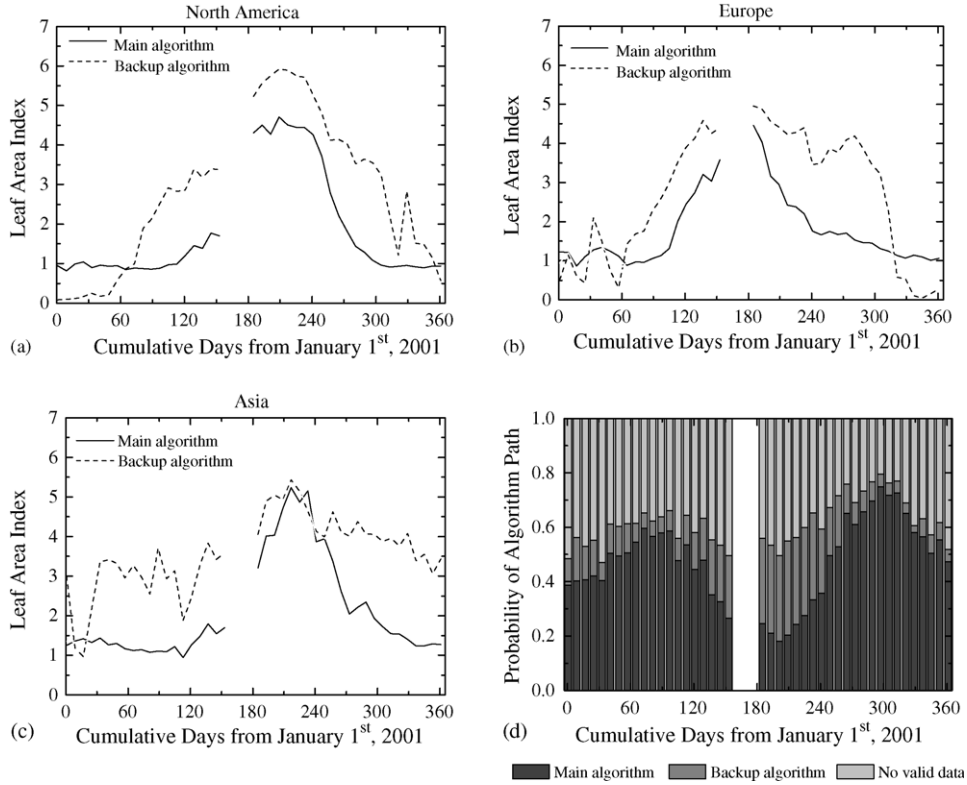

Fig. 1. Annual course of Terra MODIS Collection 3 LAI product during year 2001 for broadleaf crops in (a) North America, (b) Europe, and (c) Asia. Results from the main and back-up algorithms are shown separately. The percentage of broadleaf crops pixels processed by the main and back-up algorithms in the Northern Hemisphere is shown in (d). The data gap during days 161–184 was due to a Terra platform failure.

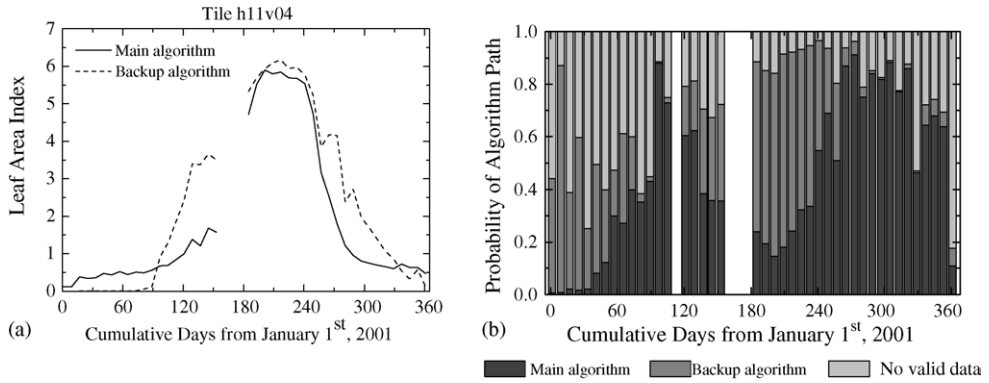

Fig. 2. (a) Annual course of Terra MODIS Collection 3 LAI product during year 2001 for broadleaf crops in tile h11v04, and (b) the percentage of broadleaf crops pixels processed by the main and back-up algorithms in tile h11v04.

biome, they nevertheless suggest that Collection 3 LAI values are very likely overestimates. The LAI seasonality from the main and back-up algorithms is different as well—the back-up algorithm produces higher LAI values during the spring and autumn. The main algorithm retrievals are as few as 20% during the summer months and most of the retrievals are from the back-up algorithm. These anomalies are similar to the ones seen at the global scale (Fig. 1), and therefore, further analysis is focused on this one tile.

4. Analysis of Collection 3 LAI anomalies

The anomalies shown in Figs. 1 and 2 raise two important questions: (1) Why does the main algorithm fail so frequently? (2) Why do the main algorithm retrievals of LAI compare so poorly with observations?. This section is devoted to finding answers to these two questions. LAI retrievals from the main algorithm depend critically on the quality of surface reflectance data input to the algorithm—therefore, the surface reflectance product is first analyzed (Section 4.1). An investigation of algorithm performance in terms of its retrieval success (Section 4.2) and quality (Section 4.3) provides the answer to the two questions raised above—a mismatch between modeled and measured reflectances (Section 4.4).

4.1. Uncertainties in surface reflectance product

The precision of measurements ($p_1, p_2, \ldots, p_n$) of a variable (P) may be characterized by the standard deviation or by the coefficient of variation (Δ):

$$\Delta = \frac{M}{S} \quad (1)$$

where M is the mean of measurements ($p_1, p_2, \ldots, p_n$) and S is the standard deviation of measurements ($p_1, p_2, \ldots, p_n$). Precision typically refers to a particular value of the variable. Uncertainty refers to precision over a range of values of the variable. The goal here is to estimate the magnitude of uncertainty in the MODIS surface reflectance product relevant to this study. To this end, daily surface reflectance data for the period July 20–27, 2001 from tile h11v04 are employed in this analysis.

The quality of MODIS surface reflectance product is reported as high, intermediate, poor due to cloud effects, and poor for other reasons (WWW2). The broadleaf crop pixels in tile h11v04 are grouped into pixels with "good quality" data if there are at least four daily surface reflectances of high or intermediate quality during the 8-day period between 20 and 27 July 2001. Likewise, the pixels with "poor quality" data are those with at least four daily surface reflectances of quality poor due to cloud effects or poor for other reasons. Uncertainties in reflectances from pixels with good quality data will therefore be due to incomplete atmospheric correction and uncertainties in reflectances from pixels with poor quality data will be due to improper cloud screening and instrumental anomalies. For the time being, it is assumed that the surface is unchanged over the measurement period of 8 days and that the solar and measurement geometry is identical from day to day for all pixels in the tile. The coefficient of variation for one "good (poor) quality" pixel is calculated from high/intermediate (poor) quality daily surface reflectances during the 8-day period.

The histograms of reflectance uncertainties for red and near-infrared channels, evaluated as coefficients of variation, for good and poor quality data in tile h11v04 are shown in Fig. 3a and b, respectively. The histograms for good (poor) quality data show peaks at 13% (59%)

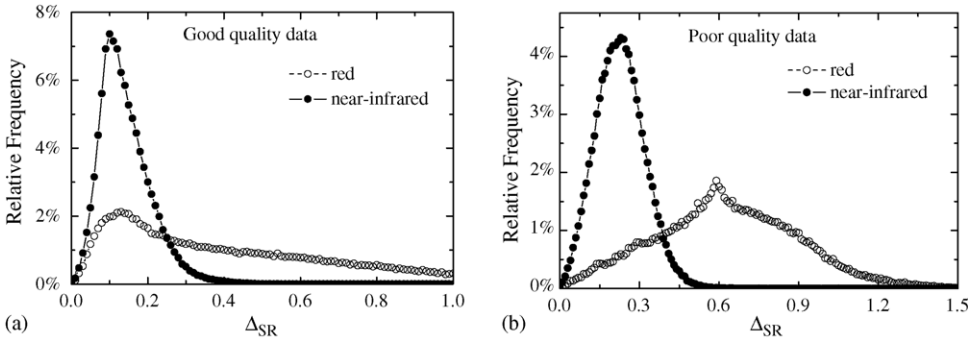

Fig. 3. Histograms of coefficients of variation (Δ_{SR}) at red and near-infrared bands for good quality data (a) and for poor quality data (b). Broadleaf crop pixels in tile h11v04 are grouped into pixels with "good quality" data if there are at least four daily surface reflectances of high or intermediate quality during the 8-day period between 20 and 27 July 2001. Likewise, the pixels with "poor quality" data are those with at least four daily surface reflectances of quality poor due to cloud effects or poor for other reasons.

for red and at 10% (23%) for near-infrared channels. The mean uncertainties (coefficients of variation) for good (poor) quality data are 44% (63%) at red and 14% (23%) at near-infrared bands. As expected, the uncertainty level of poor quality data is higher than good quality data. The main algorithm may be expected to fail if the red and near-infrared uncertainties are greater than the threshold value (20%) set in the algorithm.

Note that these uncertainty levels are subject to the assumption of invariant surface and measurement geometry. While the surface may be reasonably assumed to be unchanged over a period of 8 days, the solar and view angles change from day to day and from pixel to pixel in the tile. Reflectance variations due to changing geometry are not part of product uncertainty. Therefore, these variations must be characterized, as discussed below.

The variation in solar zenith angle at the time of measurement for both good and poor quality data during this 8-day period is negligibly small, about 10% (Fig. 4a). The variation in view zenith angle is, however, large (Fig. 4b). The histograms show two peaks for good quality data and none for poor quality data. Uncertainties in good quality surface reflectances in the red channel average 38%, 42%, and 46% when variations in view zenith angle average less than 20%, 30–40%, and 85–95% (Fig. 4c). These reflectance uncertainties are comparable to the mean uncertainty (44%) shown in Fig. 3a. Likewise, the uncertainties in poor quality surface reflectances in the red channel average 58%, 63%, and 68% when variations in view zenith angle average less than 20%, 30–40%, and 85–95% (Fig. 4d). Again, these uncertainties are comparable to the mean uncertainty (63%) shown in Fig. 3b. Therefore, we conclude that variations in measurement geometry contributed little to the uncertainty in the surface reflectance product.

The uncertainties levels in both good quality data (44% at red) and poor quality data (63% at red, 23% at near-infrared) are greater than the threshold values (20%) set in the MODIS LAI/FPAR algorithm. The main algorithm will fail in all such cases. Does this explain why there are too few main algorithm retrievals of LAI? Perhaps not, as these uncertainties levels may not be representative of the global reflectance product for this biome. Even if they were, it does not explain why the main algorithm retrievals compare poorly with field measurements. Therefore, a further investigation of algorithm performance as a function of input reflectance uncertainty is needed.

4.2. Main algorithm success rate

Pixels with good quality reflectance data, that is, pixels with at least four daily observations of high or intermediate quality surface reflectances during the 8-day period between 20 and 27 July 2001, were further sub-divided in two classes—those with uncertainties less than 12% and greater than 12%. Likewise, the pixels with poor quality data resulted in two additional groups. The four subsets are abbreviated as GL, GH, PL, and PH. The first character indicates the quality of the pixels, good (G) or poor (P). The second character refers to the uncertainty level, low $\delta_{SR} \leq 12\%$ (L), or high (H) $\delta_{SR} > 12\%$.

The main LAI/FPAR algorithm was executed with reflectance data from these four groups. The percentage of pixels for which the main algorithm produces a retrieval is defined as the retrieval index. This index characterizes the spatial coverage of the product and not its precision. The retrieval indices for the subsets GL,

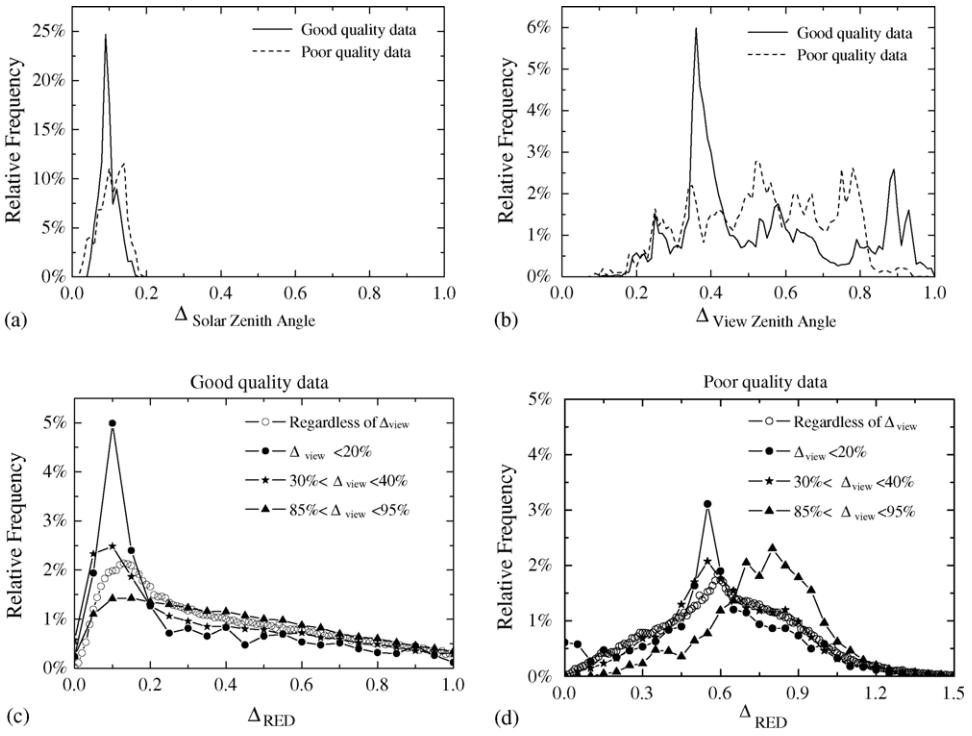

Fig. 4. (a) Histograms of coefficients of variation of solar zenith angle and view zenith angle (b) for good and poor quality data. Uncertainties in red reflectance for view zenith angle variations less than 20%, 30–40% and 85–95% are shown in (c) for good quality data and (d) for poor quality data.

GH, PL, and PH are 16.5%, 11.8%, 0.01%, and 1.7%, respectively. As expected, the main algorithm performs better with good quality input data. Likewise, the retrieval index is higher for good quality data with low uncertainties than for good quality data with high uncertainties. It is also noteworthy that the main algorithm fails as expected in the case of poor quality with low uncertainties. Nevertheless, the retrieval index for good quality data with low uncertainties is low, only about 16.5%. What is the upper limit for the retrieval index? To answer this question, the following analysis was performed.

The good quality data were divided into narrow classes with respect to uncertainties in surface reflectances (δ_{SR}) and the main algorithm was executed on these narrow groups of data. The regression curve $\overline{RI} = E(RI, \Delta_{SR} = \delta_{SR})$ of the retrieval index (RI) with respect to uncertainty of surface reflectance was evaluated. Here $E(\text{RI}, \Delta_{SR} = \delta_{SR})$ is the expectation of RI for the condition Δ_{SR} takes the value δ_{SR} (Fig. 5a). As expected, the retrieval index is a decreasing function of input data uncertainties. The maximum retrieval index of about 17% is achieved when $\delta_{SR} \leq 10\%$. These results indicate the main algorithm success rate to be only 17% for highly accurate surface reflectances. This suggests a problem with the algorithm. These results are consistent with those seen at the global and tile scale (Figs. 1d and 2b).

4.3. Quality of main algorithm retrievals

The quality of retrievals from the main algorithm is another measure of algorithm performance. Specifically, it is of interest to assess the relation between input reflectance data quality and output LAI quality. The coefficient of variation of retrieved LAI values (δ_{LAI}) during the 8-day period was calculated for each pixel, separately from the subsets of good and poor quality pixels, and taken as a measure of uncertainties in LAI retrievals. The variation in LAI values due to uncertainties in good quality surface reflectances is approximately 10% (Fig. 5b). The histogram of retrievals from poor quality pixels is wide, without obvious peaks, indicating low retrieval quality (Fig. 5b). Thus, there is a good correspondence between input and output uncertainties. The following analysis was performed to formalize this relationship.

Pixels with both good and poor quality data were split into narrow classes with respect to δ_{SR} of the red band. The coefficient of variation of LAI, Δ_{LAI}, was calculated

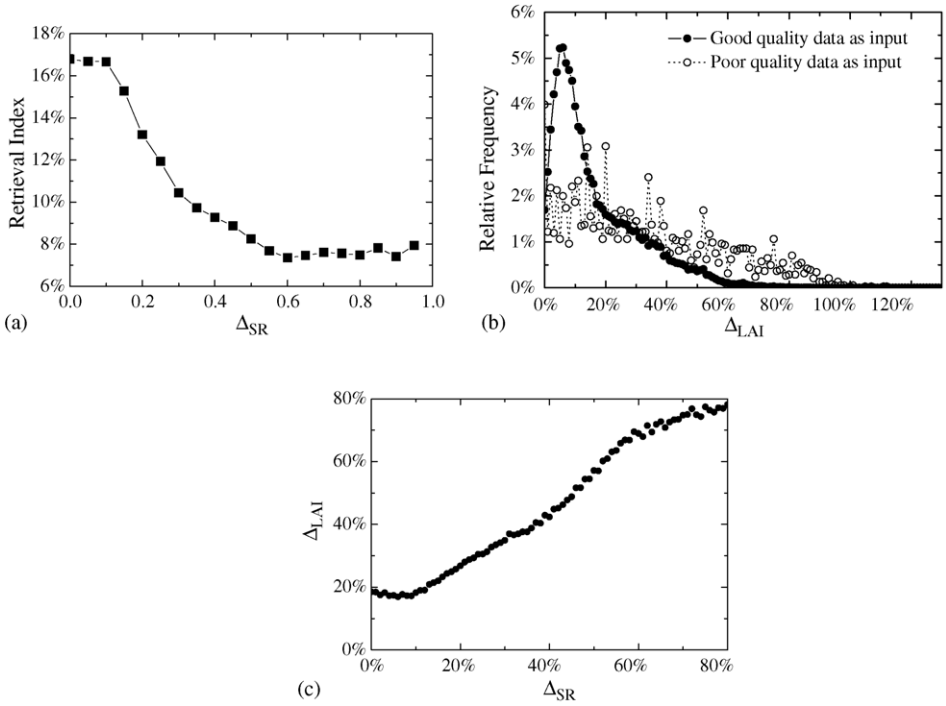

Fig. 5. Impact of input reflectance uncertainties on retrieval index and quality. The percentage of pixels for which the main algorithm produces a retrieval is defined as the retrieval index. (a) Shows decreasing retrieval index with increasing uncertainties in surface reflectances (Δ_{SR}). (b) Shows the histogram of the coefficient of variation of LAI (Δ_{LAI}) derived from good and poor quality data. The positive relationship between uncertainties in LAI retrievals (Δ_{LAI}) and uncertainties in input surface reflectances (Δ_{SR}) is shown in (c).

for each pixel. Then Δ_{SR} and Δ_{LAI} were used to derive the regression curve $\delta_{LAI} = E(\Delta_{LAI}, \Delta_{SR} = \delta_{SR})$ of Δ_{LAI} with respect to variations in surface reflectance (Fig. 5c). The resulting relationship indicates that output LAI uncertainty is nearly constant, about 20%, when input reflectance uncertainties are less than 15%. Above this input uncertainty threshold, output uncertainties are linearly related to input uncertainties. This suggests that the upper limit of Terra MODIS LAI product precision is about 80% for broadleaf crops.

4.4. Main algorithm deficiencies

The analyses presented above (Sections 4.2 and 4.3) indicate the main algorithm retrievals to be sensitive to the quality of input surface reflectances. The algorithm fails as expected in the case of poor quality reflectances. However, the low success rates in cases of good quality reflectances suggest a renewed look at the main algorithm.

The main LAI/FPAR algorithm uses biome-specific Look-Up-Tables which contain modeled canopy radiation variables that together with measured surface reflectances and their uncertainties generate LAI and FPAR retrievals. The Collection 3 LAI/FPAR products were generated with at-launch Look-Up-Tables based on reflectance data from the sea-viewing wide field-of-view sensor (SeaWiFS) (Tian et al., 2000). This could potentially be a reason for the poor performance of the main algorithm.

The average reflectance of broadleaf crops calculated from MODIS surface reflectance data from July 20 to 27, 2001, in tile h11v04 is 0.056 at red and 0.48 at near-infrared. The comparable values from SeaWiFS data, from July 1998, are 0.065 at red and 0.32 at near-infrared (Tian et al., 2000). The red reflectance values are comparable but the mean MODIS near-infrared reflectance is 50% higher than the SeaWiFS value. The near-infrared reflectance should decrease as the spatial resolution decreases from 1 km (MODIS) to 8 km (SeaWiFS) according to Tian et al. (2000). However, a 50% difference is beyond what can be expected from resolution considerations alone, and may be due to different sensors and atmospheric correction algorithms.

The 50% data density contour of good quality data, defined as data from those pixels with at least four daily observations of high or intermediate quality surface reflectances during the 8-day period between 20 and 27 July 2001, occupies the space bounded by $0.02 \leq \text{red} \leq 0.07$ and $0.32 \leq \text{near-infra red} \leq 0.58$ in the

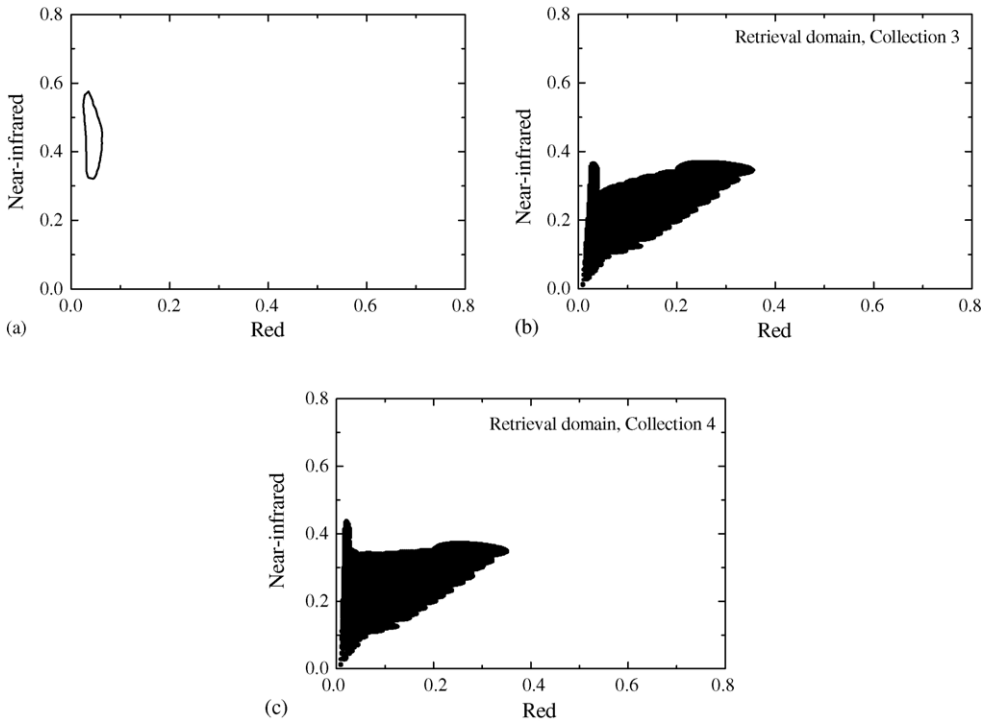

Fig. 6. (a) Shows the 50% data density contour of good quality data in the red–near-infarred space. The distribution of broadleaf crop pixels retrieved with the Collection 3 main algorithm is shown in (b). About 10% of the MODIS data contour region (a) overlaps with the retrieval domain in the Collection 3 algorithm (b). This mismatch between the simulated and MODIS reflectances is thus the main reason for the observed Collection 3 LAI anomalies. The retrieval domain for Collection 4 algorithm is shown in (c). The overlap between Collection 4 retrieval domain and the 50% MODIS data density contour is now 34%.

red–near-infrared space (Fig. 6a). That is, fully 50% of the data are contained in the space enclosed by this contour line. Only about 10% of this 50% contour region overlaps with the SeaWiFS-based retrieval domain in the Collection 3 algorithm (Fig. 6b). Most of the MODIS surface reflectance data fall in the high LAI region. Therefore, the main algorithm fails frequently and when it produces a retrieval, the LAI values are over-estimates compared to true values. This mismatch between the simulated and MODIS reflectances is thus the main reason for the observed Collection 3 LAI anomalies.

5. Algorithm refinements and the Collection 4 products

The analyses presented in Section 4 indicate that the reason why the main algorithm fails and why the retrieved LAI values are over-estimates compared to observations is the mismatch between the modeled and observed MODIS surface reflectances (Fig. 6a and b). Therefore, the Look-Up-Table entries were revised for broadleaf crops based on Collection 3 MODIS reflectances—this procedure is similar to that described in Tian et al. (2000, 2002). The single scattering albedos for red and NIR bands were tuned based on MODIS data to maximize the overlap between modeled and observed surface reflectances. The resulting retrieval domain for the Collection 4 algorithm is shown in Fig. 6.

The biome classification map accompanying the algorithm was also updated. Significant misclassification between broadleaf crops (biome 3) and grasslands (biome 1), seen in the map used for Collection 3 retrievals, are now corrected in the new classification map. It should be noted that biome misclassification might have a two-fold effect—a direct effect, whereby a misclassification may result in the selection of a wrong Look-Up-Table during the retrieval, and an indirect effect, through the algorithm calibration procedure when the Look-Up-Tables are developed.

The algorithm also benefited from improvements to the upstream algorithms—calibration, cloud screening, atmospheric correction, etc. In addition, the compositing scheme was revised as follows. Amongst the set of LAI/FPAR values from the 8-day compositing period, the LAI/FPAR pair corresponding to the maximum FPAR value was selected to represent the 8-day

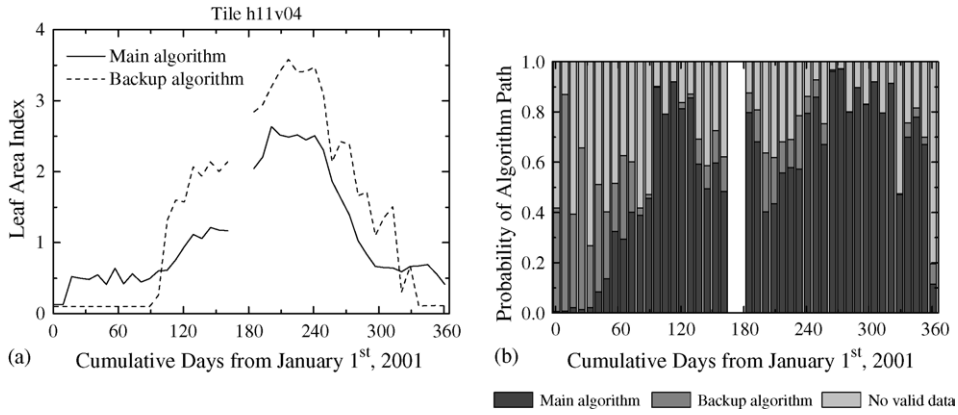

Fig. 7. (a) Annual course of Terra MODIS Collection 4 LAI product during year 2001 for broadleaf crops in tile h11vo4 and (b) the percentage of broadleaf crops pixels processed by the main and back-up algorithms in tile h11v04.

composited MODIS LAI product in Collections 1–3. This scheme leads to poor quality compositing results when back-up retrievals overwhelm main algorithm retrievals because the back-up algorithm retrievals are unreliable (Fig. 5b). This compositing scheme was changed in Collection 4 to select the LAI/FPAR pair corresponding to the maximum FPAR value generated by the main algorithm. The back-up algorithm retrievals are selected only when no main algorithm retrievals are available during the compositing period.

The above-mentioned changes were implemented in the Collection 4 algorithm which was then integrated

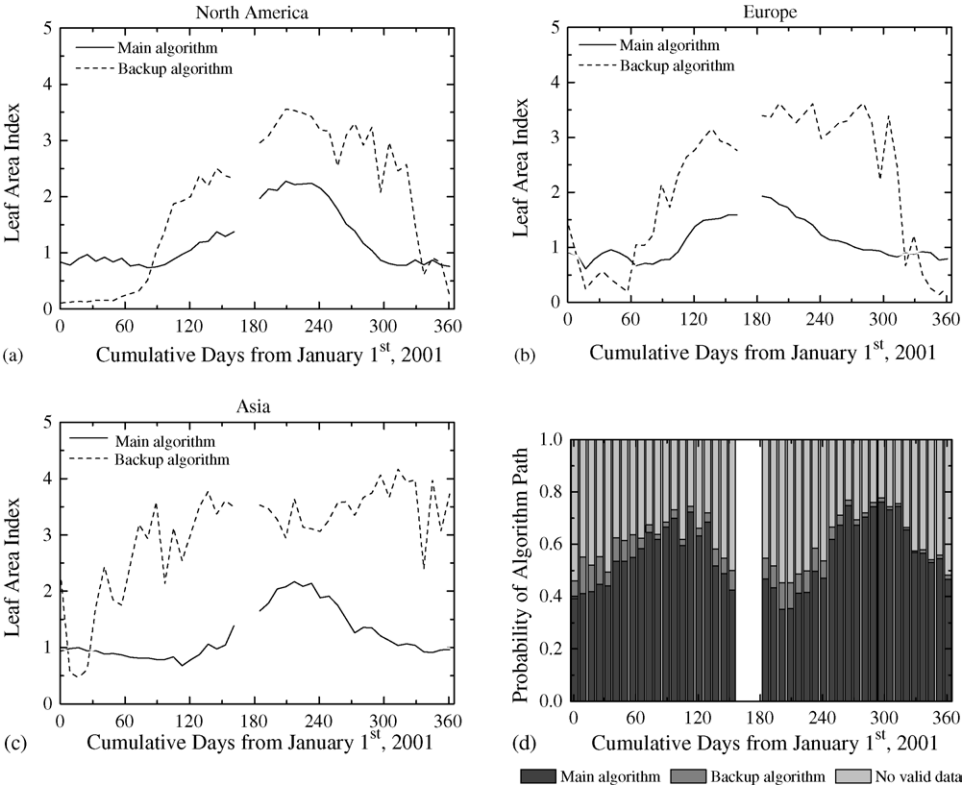

Fig. 8. Annual course of Terra MODIS Collection 4 LAI product during year 2001 for broadleaf crops in (a) North America, (b) Europe, and (c) Asia. Results from the main and back-up algorithms are shown separately. The percentage of broadleaf crops pixels processed by the main and back-up algorithms in the Northern Hemisphere is shown in (d). The data gap during days 161–184 was due to a Terra platform failure.

into the MODIS processing system to produce the Collection 4 products. This processing started in January 2003 as two streams—one forward and one re-processing of the existing data archive. The resulting products constitute the latest version and represent the entire MODIS time series (February 2000 to the present).

The Collection 4 broadleaf crops LAI product is now analyzed both for the Bondville tile (Fig. 7) and the Northern Hemisphere (Fig. 8) in order to ascertain whether the anomalies seen in Collection 3 (Figs. 1 and 2) have been satisfactorily resolved. The retrievals show peak summer LAI values of about 2–3 from the main algorithm and 3–4 from the back-up algorithm. These values compare better with seasonal maximum LAI of 4 measured near the Bondville flux tower site and values of 2.5 (July 2000) and 3.6 (August 2000) reported by Cohen et al. (2003).

The Collection 4 retrievals from the main algorithm are significantly higher, over 80% of pixels with valid data, during the summer months, and represent a major fraction of the retrievals during the growing season (Figs. 7b and 8d compared to Figs. 1d and 2b). Differences in LAI seasonality between the main and back-up algorithm persisted in Collection 4 products. Clearly, the retrievals from the back-up algorithm should use with caution, as these are produced with uncertain input data and therefore not suitable for validation studies (Running et al., 1999). Based on results presented in Figs. 7 and 8, it is concluded that the two anomalies noted in Collection 3 broadleaf crop LAI retrievals (Figs. 1 and 2) have been satisfactorily resolved in the Collection 4 retrievals. The validation of Collection 4 LAI and FPAR products is reported in various journal articles (Tan et al., 2005; Wang et al., 2004; Cohen et al., 2003).

6. Conclusions

This paper reports on investigations about the Terra MODIS LAI product for broadleaf crops, one of six biome classes implemented in the LAI/FPAR algorithm. The following conclusions can be drawn based on the results presented in this article. (1) Three LAI anomalies are seen in the Collection 3 product—(a) high LAI values during the peak growing season, (b) differences in LAI seasonality between the main and back-up algorithms, and (c) too few retrievals from the main algorithm during the summer period when the crops are at full flush. (2) The quality of LAI generated by the algorithm depends critically on the quality of surface reflectance data input to the algorithm. (3) The algorithm frequently fails or generates LAI overestimates because of a mismatch between modeled and measured reflectances. Therefore, the Look-Up-Tables accompanying the algorithm were revised for this biome class. (4) The anomalies seen in Collection 3 LAI product are satisfactorily resolved in Collection 4 produced with the revised Look-Up-Tables—the main algorithm generates over 80% of the retrievals from pixels with valid input surface reflectances. (5) Finally, the few retrievals in the Collection 4 product from the back-up algorithm should be used with caution as these are generated from highly uncertain surface reflectances and as such are not suitable for validation studies.

Acknowledgements

This work was funded by the NASA Earth Science Enterprise under the MODIS contract to Boston University. The authors thank Bondville FLUXNET group for making their field data available. The authors also acknowledge the contributions of several individuals to the MODIS land data processing, notably Drs. El Saleous, Justice, Roy, Vermote, and Wolfe.

Appendix A. WWW sites

WWW1: FLUXNET sites, http://daac.ornl.gov/FLUXNET/.

WWW2: MODIS surface reflectance products, http://modis-land.gsfc.nasa.gov/MOD09/MOD09ProductInfo/MOD09Level2G500m.htm.

References

Cohen, W.B., Maiersperger, T.K., Yang, Z., Gower, S.T., Turner, D.P., Ritts, W.D., Berterretche, M., Running, S.W., 2003. Comparisons of land cover and LAI estimates derived from ETM+ and MODIS for four sites in North America: a quality assessment of 2000/2001 provisional MODIS products. Remote Sens. Environ. 88, 233–255.

Fensholt, R., Sandholt, I., Rasmussen, M.S., 2004. Evaluation of MODIS LAI, fAPAR and the relation between fAPAR and NDVI in a semi-arid environment using in situ measurements. Remote Sens. Environ. 91, 490–507.

Friedl, M.A., McIver, D.K., Hodges, J.C.F., Zhang, X.Y., Muchoney, D., Strahler, A.H., Woodcock, C.E., Gopal, S., Schneider, A., Cooper, A., 2002. Global land cover mapping from MODIS: Algorithms and early results. Remote Sens. Environ. 83, 287–302.

Huemmrich, K.F., Privette, J.L., Mukelabai, M., Myneni, R.B., Knyazikhin, Y., 2005. Time-series validation of MODIS land biophysical products in a Kalahari Woodland. Africa. Int. J. Remote Sens. 26, 4381–4398.

Justice, C.O., Townshend, J.R.G., Vermote, E.F., Masuoka, E., Wolfe, R.E., Saleous, N., Roy, D.P., Morisette, J.T., 2002. An overview of MODIS land data processing and product status. Remote Sens. Environ. 83, 3–15.

Knyazikhin, Y., Martonchik, J.V., Myneni, R.B., Diner, D.J., Runing, S.W., 1998. Synergistic algorithm for estimating vegetation canopy leaf area index and fraction of absorbed photosynthetically active radiation from MODIS and MISR data. J. Geophys. Res. 103, 32257–32275.

Morisette, J.T., Privette, J.L., Justice, C.O., 2002. A framework for the validation of MODIS land products. Remote Sens. Environ. 83, 77–96.

Myneni, R.B., Hoffman, S., Knyazikhin, Y., Privette, J.L., Glassy, J., Tian, Y., Wang, Y., Song, X., Zhang, Y., Smith, G.R., Lotsch, A., Friedl, M., Morisette, J.T., Votava, P., Nemani, R.R., Running, S.W., 2002. Global products of vegetation leaf area and fraction absorbed PAR from year one of MODIS data. Remote Sens. Environ. 83, 214–231.

Myneni, R.B., Nemani, R.R., Running, S.W., 1997. Estimation of global leaf area index and absorbed par using radiative transfer models. IEEE Trans. Geosci. Remote Sens. 35, 1380–1393.

Privette, J.L., Myneni, R.B., Knyazikhin, Y., Mukufute, M., Roberts, G., Tian, Y., Wang, Y., Leblanc, S.G., 2002. Early spatial and temporal validation of MODIS LAI product in Africa. Remote Sens. Environ. 83, 232–243.

Running, S.W., Collatz, G.J., Washburne, J., Sorooshian, S., Dunne, T., Dickinson, R.E., Shuttleworth, W.J., Vorosmarty, C.J., Wood, E.F., 1999. Land ecosystems and hydrology. In: King, M.D. (Ed.), EOS Science Plan. National Aeronautics and Space Administration, Greenbelt, pp. 197–259.

Sellers, P.J., Randall, D.A., Betts, A.K., Hall, F.G., Berry, J.A., Collatz, G.J., Denning, A.S., Mooney, H.A., Nobre, C.A., Sato, N., Field, C.B., Henderson-sellers, A., 1997. Modeling the exchanges of energy, water, and carbon between continents and the atmosphere. Science 275, 502–509.

Tan, B., Hu, J., Zhang, P., Huang, D., Shavanov, V.N., Weiss, M., Knyazikhin, Y., Myneni, R.B., 2005. Validation of MODIS LAI product in croplands of Alpilles, France. J. Geophys. Res. 110, D0110710.1029/2004JD004860.

Tian, Y., Wang, Y., Zhang, Y., Knyazikhin, Y., Bogaert, J., Myneni, R.B., 2002. Radiative transfer based scaling of LAI/FPAR retrievals from reflectance data of different resolutions. Remote Sens. Environ. 84, 143–159.

Tian, Y., Zhang, Y., Knyazikhin, Y., Myneni, R.B., Glassy, J., Dedieu, G., Running, S.W., 2000. Prototyping of MODIS LAI and FPAR algorithm with LASUR and LANDSAT data. IEEE Trans. Geosci. Remote Sens. 38, 2387–2401.

Wang, Y., Tian, Y., Zhang, Y., El-Saleous, N., Knyazikhin, Y., Vermote, E., Myneni, R.B., 2001. Investigation of product accuracy as a function of input and model uncertainities: case study with SeaWiFS and MODIS LAI/FPAR algorithm. Remote Sens. Environ. 78, 296–311.

Wang, Y., Woodcock, C.E., Buermann, W., Stenberg, P., Voipio, P., Smolander, H., Hame, T., Tian, Y., Hu, J., Knyazikhin, Y., Myneni, R.B., 2004. Evaluation of the MODIS LAI algorithm at a coniferous forest site in Finland. Remote Sens. Environ. 91, 114–127.